exact numerical evaluation of all the microscopic contributions to $\Gamma_{12}-\Gamma_{25'}$ splitting (except $2s$-$3d$ covalency). Because of spatial symmetry, the $3d$-$2p$ transfer plays no role. The resulting calculated value of the Γ_{12}-$\Gamma_{25'}$ splitting is negative (e_g lower) and the crystal field contribution is rather insensitive to the wave functions.

It is interesting to compare our results with the recent augmented plane-wave (APW) calculation of the band structure of ReO_3 by Mattheiss.[12] The crystallographic and electronic structures of ReO_3 are very similar to that of $SrTiO_3$ and $KTaO_3$, and consequently, the basic qualitative results of band calculation are expected to be the same for all three materials. Mattheiss calculates a value[12] of the $\Gamma_{12}-\Gamma_{25'}$ splitting in ReO_3 which is positive and equal to 3.9 eV, 2.6 eV being due to the $5d$-$2s$ covalency and 1.3 eV due to crystal potential. The latter contribution, which was calculated using the corrections to the "muffin-tin" potential is equivalent to the diagonal term discussed in this paper and which for $SrTiO_3$ turns out to be negative. The discrepancy is certainly due to the use of different potentials. Because the corrections to the muffin-tin potential (atomic Coulomb interaction and Slater average exchange potential) do not mirror sufficiently accurately the microscopic character of the crystal field potential, the APW calculation of this particular problem of crystal field contribution to the $\Gamma_{12}-\Gamma_{25'}$ splitting should be compared with the quantitiative theory outlined above. The same is true for the APW calculation of Γ_{12}-$\Gamma_{25'}$ splitting in $SrTiO_3$ mentioned briefly in Ref. 12. The results of such an analysis may be even more important in transition-metal oxide with rocksalt structure (TiO and VO), because in these materials, the d functions at $k=0$ are orthogonal to both $2p$ and $2s$ oxygen wave functions and the positive contribution of $2s$-$3d$ covalency is missing.

ACKNOWLEDGMENT

The author is grateful to Professor R. Orbach for many suggestions and interest in this work and Professor T. Holstein, Professor P. Pincus, Professor E. Simanek, Professor Nai Li Huang, and Professor N. Rivier for helpful discussions.

[5]S. H. Wemple, Phys. Rev. 137, A1575 (1965).
[6]D. M. Hannon, Phys. Rev. 164, 366 (1967).
[7]J. W. Conley and G. D. Mahan, Phys. Rev. 161, 681 (1967).
[8]W. S. Baer, Phys. Rev. Letters 16, 729 (1966).
[9]H. P. R. Frederikse, W. R. Hosler, and W. R. Thurber, Phys. Rev. 143, 648 (1966).
[10]S. Sugano and R. G. Shulman, Phys. Rev. 130, 517 (1963).
[11]H. P. R. Frederikse and G. A. Candela, Phys. Rev. 147, 583 (1966).
[12]L. F. Mattheiss, Phys. Rev. 181, 987 (1969).

†Work supported in part by the National Science Foundation.

*On leave from the Institute of Radio Engineering and Electronics, Czechoslovak Academy of Science, Prague, Czechoslovakia.

[1]L. S. Senhouse, G. E. Smith, and M. V. De Paolis, Phys. Rev. Letters 15, 776 (1965).
[2]W. R. Hosler and H. P. R. Frederikse, Solid State Commun. 7, 1443 (1969).
[3]Z. Sroubek, Solid State Commun. 7, 1561 (1969).
[4]A. H. Kahn and A. J. Leyendecker, Phys. Rev. 135, A1321 (1964).

PHYSICAL REVIEW B VOLUME 2, NUMBER 8 15 OCTOBER 1970

Transverse Magnetoconductivity in n-Type Germanium†*

P. K. Govind‡ and S. C. Miller
Department Of Physics and Astrophysics, University of Colorado, Boulder, Colorado 80302
(Received 22 April 1970)

A quantum-mechanical calculation of transverse magnetoresistance is made for an electron gas with anisotropic effective mass. For acoustic-phonon scattering, numerical calculations are made with parameters appropriate to the conduction band of n-Ge in the temperature range 30–77 °K with magnetic fields up to 200 kG. For high magnetic fields there is a quantitative disagreement between theory and experiment which is not understood at present.

I. INTRODUCTION

There has been a relatively small amount of experimental work on high magnetic field transverse magnetoresistance in semiconductors. This is largely due to the belief of many investigators that effects of inhomogeneities are greater than those of fundamental scattering mechanisms. However, the experiments of Gallagher and Love[1] suggested that inhomogeneity effects might not be

so important. More recently, Baranskii and Babich[2] have made a detailed investigation of the influence of various inhomogeneities in high-field transverse magnetoresistance. They conclude that there is little correlation between inhomogeneities and the magnetoresistance. It is, therefore, of interest to see if calculated transverse magnetoresistance agrees with experiment. In this paper such a calculation is made for n-germanium assuming acoustic-phonon scattering of the electrons.

Electrical transport in the presence of magnetic fields where the Landau quantization is important has been studied by a number of authors.[3-8] Most of these investigations are limited to the extreme quantum limit (strong magnetic fields) where the electron cyclotron angular frequency ω_c is large enough so that $\hbar\omega_c/kT \gg 1$; also, in this limit ω_c is greater than $1/\tau$ the reciprocal of the relaxation time. The general form of the expression for current derived in most published works presents divergence difficulties in summing over energy states. Various authors have used special cutoff mechanisms to offset this difficulty. In any case, regardless of the formalism few detailed calculations have been made using the properties of real semiconductors.

A formalism in which $1/\tau$ is not assumed negligible compared to ω_c was suggested by Argyres.[9] This not only makes the theory applicable to low as well as high magnetic fields, but also eliminates the divergence difficulties. In this paper we extend the approach of Argyres[9] and of Adams and Holstein[3] (AH) to include the case of anisotropic energy surfaces. Numerical calculations are made for n-Ge as a practical application of the theory.

In Sec. II, the general formalism is developed. Sections III and IV deal with the application of the theory to n-type germanium. Numerical results on n-Ge are displayed graphically and discussed in Sec. V.

II. GENERAL FORMALISM

The quantity of physical interest is the electric current. The equation that will be used in obtaining the statistical average of the current density is

$$\langle \vec{j} \rangle = \mathrm{Tr}\,(\rho \vec{j}) \ . \tag{2.1}$$

Here $\vec{j}$ is the current operator and ρ is the density-matrix operator that depends on the total Hamiltonian of the system. The trace is taken over a complete set of states of the system considered. In this work, we will treat electron-phonon scattering in the presence of crossed electric and magnetic fields. Our first task, therefore, is to find the density matrix ρ, assuming that the scattering interaction V is small compared with the rest of the single-particle Hamiltonian.

The density matrix ρ will evolve according to the Liouville equation

$$i\hbar \frac{d\rho}{dt} = [H + V, \rho] \ . \tag{2.2}$$

We will assume that at $t = 0$, the interaction potential V is switched on, and that prior to this time the system is in thermal equilibrium. We express this by saying

$$\rho_{t=0} = \rho(0) = f \ , \tag{2.3}$$

where $f(\epsilon) = [e^{(\epsilon-\mu)/kT} + 1]^{-1}$ is the Fermi distribution function with μ as the Fermi energy. If $p(s)$ is s times the Laplace transform of $\rho(t)$, Eq. (2.2) is equivalent to

$$i\hbar s p(s) = [H + V, p(s)] + i\hbar s \rho(0) \ . \tag{2.4}$$

As $t \to \infty$, we expect ρ to approach a steady state. For such a function, s times its Laplace transform approaches the function as $t \to \infty$ if the limit $s \to 0$ is taken. Following AH, we assume

$$p_{\nu\nu'} = f_\nu \delta_{\nu\nu'} + G_{\nu\nu'} + J_{\nu\nu'} \ . \tag{2.5}$$

Here, the subscripts stand for the matrix elements between the states ν and ν'. The eigenfunctions and eigenvalues will be discussed in Sec. III. For the general discussion of this section, it is sufficient to point out that a state such as ν is characterized by a set of quantum numbers (n, k_y, k_z), typical of the eigenvalue problem. The quantity $f_\nu \delta_{\nu\nu'}$ is the initial value of the density matrix and $G_{\nu\nu'} + J_{\nu\nu'}$ is s times the Laplace transform of the correction to the density matrix due to scattering. $G_{\nu\nu'}$ is defined to be that part of $p(s)$ for which the states ν and ν' are characterized by the same wave number $(k_y = k_y', k_z = k_z')$. The elements $J_{\nu\nu'}$ are defined to be equal to zero in this case. The transform p is broken up in this form because the matrix elements of the current operators that determine the conductivity are found to be diagonal in the k's with $n' = n \pm 1$ (see Sec. III). We will effect an expansion in powers of the interaction potential V. Combination of Eqs. (2.4) and (2.5) gives

$$-i\hbar s(G_{\nu\nu'} + J_{\nu\nu'}) = [G, H]_{\nu\nu'} + [J, V]_{\nu\nu'} + [G, V]_{\nu\nu'} + [J, H]_{\nu\nu'} + [f, V]_{\nu\nu'} \ . \tag{2.6}$$

From Eq. (2.6), we find

$$-i\hbar s J_{\nu\nu'} = -\epsilon_{\nu\nu'} J_{\nu\nu'} + f_{\nu\nu'} V_{\nu\nu'} + [G, V]_{\nu\nu'} + [J, V]_{\nu\nu'} \ . \tag{2.7}$$

In this equation, $\epsilon_{\nu\nu'}$ stands for the energy difference $\epsilon_\nu - \epsilon_{\nu'}$ and $f_{\nu\nu'}$ will mean $f_\nu - f_{\nu'}$. We look for a solution of J to lowest order in V. To

this order Eq. (2.7) gives us

$$J_{\nu\nu'} = \{f_{\nu\nu'} V_{\nu\nu'} + [G, V]_{\nu\nu'}\}/(\epsilon_{\nu\nu'} - i\hbar s) \ . \qquad (2.8)$$

On the other hand, terms diagonal in k_y and k_z in Eq. (2.6) give

$$-i\hbar s\, G_{nn'} = -\epsilon_{nn'} G_{nn'} + [J, V]_{nn'}$$
$$= -\epsilon_{nn'} G_{nn'} + \textstyle\sum_\lambda (J_{n\lambda} V_{\lambda n'} - V_{n\lambda} J_{\lambda n'}). \qquad (2.9)$$

The summation index λ stands for a set of quantum numbers $\{n'', k_y'', k_z''\}$. Substituting for J from Eq. (2.8), we can rewrite Eq. (2.9) as

$$-i\hbar s\, G_{nn'} = -\epsilon_{nn'} G_{nn'} + \sum_\lambda V_{n\lambda} V_{\lambda n'} \times \left(\frac{f_{n\lambda}}{\epsilon_{n\lambda} - i\hbar s} - \frac{f_{n'\lambda}}{\epsilon_{n'\lambda} + i\hbar s}\right)$$
$$+ \sum_\lambda \left(\frac{G_{nn'} |V_{n'\lambda}|^2}{\epsilon_{n\lambda} - i\hbar s} + \frac{G_{nn'} |V_{n\lambda}|^2}{\epsilon_{\lambda n'} - i\hbar s}\right) . \qquad (2.10)$$

Here, the nonquadratic terms in V and quadratic terms in V other than those which will lead to the form $|V_{n\lambda}|^2$ are dropped, because in an ensemble average, the random phonon phases make these terms go to zero.[3,9] Finding the limit of ρ as $t \to \infty$ by setting $s \to 0$ on the left-hand side of Eq. (2.10), we obtain after a rearrangement

$$G_{nn'} = \sum_\lambda V_{n\lambda} V_{\lambda n'} \left(\frac{f_{n\lambda}}{\epsilon_{n\lambda} - i\hbar s} - \frac{f_{n'\lambda}}{\epsilon_{n'\lambda} + i\hbar s}\right) \Bigg/ \times \left[\epsilon - \sum_\lambda \left(\frac{|V_{n\lambda}|^2}{\epsilon_{n\lambda} - i\hbar s} - \frac{|V_{n'\lambda}|^2}{\epsilon_{n'\lambda} + i\hbar s}\right)\right] . \qquad (2.11)$$

The second term in the denominator has been missing in most discussions of electrical transport by other investigators, leading to divergence difficulties. To simplify further, we will use the result

$$\lim_{s\to 0} \frac{1}{x - is} = P\left(\frac{1}{x}\right) + i\pi\delta(x) \ ,$$

with

$$P(1/x) = 1/x \quad \text{for } x \neq 0$$
$$= 0 \quad \text{for } x = 0. \qquad (2.12)$$

The principal part of $P(1/x)$ will not be used. As discussed by AH, upon changing $t \to -t$ the contributions from the principal parts do not change sign, whereas the direction of current flow is reversed. Since s changes sign with time, only terms that change sign with s can describe currents. Equation (2.11) then becomes

$$G_{nn'} = i\pi \textstyle\sum_\lambda V_{n\lambda} V_{\lambda n'} [f_{n\lambda}\delta(\epsilon_{n\lambda}) + f_{n'\lambda}\delta(\epsilon_{n'\lambda})] / \times \{\epsilon_{nn'} - i\pi \textstyle\sum_\lambda [|V_{n\lambda}|^2 \delta(\epsilon_{n\lambda}) + |V_{n'\lambda}|^2 \delta(\epsilon_{n'\lambda})]\} . \qquad (2.13)$$

Equation (2.13) represents the general perturbation approximation for the density-matrix elements and will be used to calculate the electric current in Sec. IV.

III. WAVE FUNCTIONS AND CURRENT-DENSITY-MATRIX ELEMENTS IN n-Ge.

We now specialize to the case of germanium. In germanium, the conduction-band minima are at the first Brillouin-zone boundary along the four principal diagonals [111], [$\bar{1}$11], [1$\bar{1}$1], and [11$\bar{1}$] of the reciprocal lattice.[10] The eight half-ellipsoids terminated by the plane surfaces of the Brillouin zone are equivalent to four complete ellipsoids. The transport properties which we calculate are the sum of contributions from each ellipsoid.

The effective-mass Hamiltonian for an electron in an anisotropic crystal like n-Ge in the presence of uniform electric [$\vec{E}$] and magnetic [$\vec{B}$] fields is

$$H = \sum_{i,j} \frac{\alpha_{ij}^{(\sigma)}}{2m} \left(\nu_i - \frac{eA_i}{c}\right)\left(p_j - \frac{eA_i}{c}\right) - e\vec{E}\cdot\vec{r} \ , \qquad (3.1)$$

where $\vec{A}$ is the vector potential describing the magnetic field $\vec{B}$ and e and m are the electronic charge and mass, respectively. The quantity $\alpha_{ij}^{(\sigma)}/m$ is the reciprocal mass tensor whose components depend on the orientation of the σth energy ellipsoid with respect to a chosen coordinate system (x, y, z). In the principal axis system (x', y', z') of each ellipsoid, α is a diagonal tensor; however, for the general case of an ellipsoid of revolution about the $z'^{(\sigma)}$ axis we find[11]

$$\alpha_{ij}^{(\sigma)} = \begin{pmatrix} a_{11}\cos^2\phi_\sigma + \alpha_1 \sin^2\phi_\sigma & (a_{11} - \alpha_1)\sin\phi_\sigma\cos\phi_\sigma & a_{13}\cos\phi_\sigma \\ (a_{11} - \alpha_1)\sin\phi_\sigma\cos\phi_\sigma & a_{11}\sin^2\phi_\sigma + \alpha_1\cos^2\phi_\sigma & a_{13}\sin\phi_\sigma \\ a_{13}\cos\phi_\sigma & a_{13}\sin\phi_\sigma & \alpha_{33} \end{pmatrix} , \qquad (3.2)$$

with

$$a_{11} = \alpha_1\cos^2\theta_\sigma + \alpha_3\sin^2\theta_\sigma, \quad \alpha_{33} = \alpha_1\sin^2\theta_\sigma + \alpha_3\cos^2\theta_\sigma, \quad a_{13} = (\alpha_1 - \alpha_3)\sin\theta_\sigma\cos\theta_\sigma, \quad \alpha_1 = m/m_t, \quad \alpha_3 = m/m_l \ .$$

The masses m_t and m_l are the transverse and longitudinal effective masses, respectively. Here θ_σ is the angle between the chosen z axis ($\vec{B}$) and the longitudinal principal axis ($z'^{(\sigma)}$) of the σth ellipsoid; ϕ_σ is the angle between the $x'^{(\sigma)}$ $z'^{(\sigma)}$ plane and the $zz'^{(\sigma)}$ plane. In all intermediate calculations, we will be dealing with only one ellipsoid. We first determine all our results for this ellipsoid and then obtain the corresponding quantities for the whole conduction band by summing over all the ellipsoids. The ellipsoid index σ will be suppressed in the following for convenience.

For the z axis along $\vec{B}$ and the x axis along $\vec{E}$, the gauge may be chosen such that $\vec{A} = (-Bx\alpha_{12}/\alpha_{11}, Bx, 0)$. Then, the eigenfunctions of the Hamiltonian (3.1) may be verified to be

$$\Psi_{n,k_y,k_z} = \exp[i(k_y y + k_z z) - i(\gamma_{13}k_z + \gamma_{12}k_y)x] \times \phi_n[\beta(x - x_0)] , \tag{3.3}$$

where in terms of the Hermite polynomials H_n,

$$\phi_n[\beta(x-x_0)] = [\beta/(\pi^{1/2}2^n n!)]^{1/2} \times \exp[-\tfrac{1}{2}\beta^2(x-x_0)^2]H_n[\beta(x-x_0)] , \tag{3.4}$$

with

$$\beta = \frac{(\bar{\alpha}_{22}/\alpha_{11})^{1/4}}{\lambda_m}, \quad \lambda_m = \left(\frac{c\hbar}{eB}\right)^{1/2}, \quad \gamma_{13} = \frac{\alpha_{13}}{\alpha_{11}} ,$$
$$\gamma_{12} = \alpha_{12}/\alpha_{11}, \quad \text{and} \quad \bar{\alpha}_{22} = \alpha_{22} - \alpha_{12}^2/\alpha_{11} . \tag{3.5}$$

The corresponding eigenvalues are given by

$$\epsilon_{n,k_y,k_z} = \epsilon_{n,k_z} + \tfrac{1}{2}m(cE/B)^2 + eEx_0 . \tag{3.6}$$

Here,

$$\epsilon_{n,k_z} = (n + \tfrac{1}{2})\hbar\omega^* + \hbar^2 k_z^2/2m^* \quad (n = 0, 1, 2, \ldots) , \tag{3.7}$$

with

$$\omega^* = \omega_c(\alpha_{11}\bar{\alpha}_{22})^{1/2} ,$$

where

$$\omega_c = (eB/mc) .$$

Also,

$$\frac{1}{m^*} = \frac{1}{m}\left(\alpha_{33} - \frac{\alpha_{13}^2}{\alpha_{11}}\right) - \frac{1}{2\bar{\alpha}_{22}}\left(\alpha_{22} - \frac{\alpha_{13}\alpha_{12}}{\alpha_{11}}\right)^2 \tag{3.8}$$

and

$$x_0 = -\lambda_m^2\left[k_y + \frac{1}{\bar{\alpha}_{22}}\left(\alpha_{23} - \frac{\alpha_{13}\alpha_{12}}{\alpha_{11}}\right)k_z\right] - \frac{m}{\bar{\alpha}_{22}cE}\left(\frac{cE}{B}\right)^2 . \tag{3.9}$$

The quantity $\lambda_m = (c\hbar/eB)^{1/2}$ is a length comparable to the orbit radius for the ground state $n = 0$. The distance x_0 corresponds to the x coordinate of the center of the cyclotron orbit. In Eq. (3.6), the term eEx_0 can be regarded as the average potential energy of the electron in the electric field and $\frac{1}{2}m(cE/B)^2$ the additional translational kinetic energy due to the (cE/B) drift velocity.

The electric current density is given by $\hat{j}_i = e\hat{v}_i$, where the velocity-operator components $\hat{v}_i$ are given by $(i/\hbar)[H, \vec{r}]$. The transverse current components are then found to be

$$\hat{j}_x = (e/m)(\alpha_{11}p_x + \alpha_{13}p_z + \alpha_{12}p_y) ,$$
$$\hat{j}_y = \frac{e}{m}\left[\alpha_{22}\left(p_y - \frac{eBx}{c}\right) + \frac{\alpha_{12}^2}{\alpha_{11}}\left(\frac{eB}{c}\right)x + \alpha_{12}p_x + \alpha_{23}p_z\right] . \tag{3.10}$$

With the wave functions (3.3), the matrix elements of the current operators of Eq. (3.10) are diagonal in k_y and k_z. The dependence on n is

$$(\hat{j}_x)_{n'n} = (-i\hbar e\beta\alpha_{11}/m)\{(\tfrac{1}{2}n)^{1/2}\delta_{n',n-1} - [\tfrac{1}{2}(n+1)]^{1/2}\delta_{n',n+1}\} ,$$
$$(\hat{j}_y)_{n'n} = (e\hbar/m)(\bar{\alpha}_{22}\alpha_{11})^{1/2}\beta\{[\tfrac{1}{2}(n+1)]^{1/2}\delta_{n',n+1} + (\tfrac{1}{2}n)^{1/2}\delta_{n',n-1}\} . \tag{3.11}$$

Recalling Eq. (2.1), we find the transverse components of current density to be

$$\langle j_x\rangle = \frac{ie\hbar}{\sqrt{2}m}\alpha_{11}\beta\sum_{n,k}[(n+1)^{1/2}\rho_{n+1,n} - n^{1/2}\rho_{n-1,n}] ,$$
$$\langle j_y\rangle = \frac{e\hbar}{\sqrt{2}m}(\bar{\alpha}_{22}\alpha_{11})^{1/2}\beta\sum_{n,k}[n^{1/2}\rho_{n-1,n} + (n+1)^{1/2}\rho_{n+1,n}] + e\frac{cE}{B}\sum_{n,k}\rho_{nn} . \tag{3.12}$$

We are now in a position to use Eq. (2.13) to find the electric current density. This will be done in Sec. IV for the case of acoustic-phonon scattering.

IV. ACOUSTIC SCATTERING CONDUCTIVITY

In the 30–77 °K temperature region of interest to us in this work, acoustic-phonon scattering appears to dominate in relatively pure germanium samples.[12,13] Thus, we will calculate the transverse-current components for electrons which interact with acoustic phonons in uniform crossed electric and magnetic fields. It will be assumed in the calculations that the change in the phonon distribution function from its equilibrium value is small and that the electron-electron collisions can be neglected. Also, the change in electron energy due to scattering will be taken to be much less than kT, i.e., the scattering is essentially

elastic. For $T > 20\,^{\circ}$K, this assumption is justified in Ge.[14] Only intravalley scattering will be treated since for the temperatures and magnetic fields considered here ($30 \leq T \leq 77\,^{\circ}$K, $0 \leq B \leq 200$ kG) we can neglect intervalley scattering.

For the perturbation due to lattice vibrations, we use

$$V = E_1 \sum_q Q_q q \exp(i\vec{q}\cdot\vec{r}) \quad , \tag{4.1}$$

where Q_q is an acoustic-phonon creation or annihilation operator and E_1 is the coupling constant between the electrons and the dilational waves for the phonon mode $\vec{q}$ in the Shockley-Bardeen theory.[15] The transition from an electronic state Ψ_{n,k_y,k_z} to a state $\Psi_{n',k_y',k_z'}$ via this interaction involves the matrix element squared,

$$|\langle n', k_y', k_z' | e^{i\vec{q}\cdot\vec{r}} | n, k_y, k_z \rangle|^2 = C^2 \textstyle\sum_q \delta_{k_y, k_y'+q_y} \delta_{k_z, k_z'+q_z} |J_{nn'}|^2 \quad . \tag{4.2}$$

Here $C^2 = E_1^2 kT/(2\rho_d v_s^2)$, ρ_d is the density of the crystal, and v_s is the speed of sound in the crystal. For the phonon mode $\vec{q}$

$$|J_{nn'}|^2 = \left| \int_{-\infty}^{\infty} dx\, \phi_{n'}^*[\beta(x - x_0)] \times \exp[i(q_x + \gamma_{13} q_z + \gamma_{12} q_y)x]\, \phi_n[\beta(x - x_0)] \right|^2 . \tag{4.3}$$

A useful summation formula[13] for $|J_{nn'}|^2$ is

$$\int dq_x\, dq_y\, |J_{nn'}|^2 = 2\pi/\lambda_m^2 \quad . \tag{4.4}$$

The current components can now be obtained from Eqs. (2.13) and (3.12) as

$$\langle j_x \rangle = \sqrt{2\pi}\, \frac{e\hbar}{m} \beta \alpha_{11} \sum_{n,k} (n+1)^{1/2} \sum_{\lambda} V_{n\lambda} V_{\lambda,n+1} [f_{n\lambda}\delta(\epsilon_{n\lambda}) + f_{n+1,\lambda}\delta(\epsilon_{n+1,\lambda})] \epsilon_{n,n+1} / (\epsilon_{n,n+1}^2 + \pi^2 \{ \textstyle\sum_{\lambda} [|V_{n\lambda}|^2 \delta(\epsilon_{n\lambda}) + |V_{n+1,\lambda}|^2 \delta(\epsilon_{n+1,\lambda})] \}^2) , \tag{4.5}$$

$$\langle j_y \rangle = \frac{e\hbar}{m} (\alpha_{22}\alpha_{11})^{1/2} \beta \sum_{n,k} \left[\frac{(eE/\beta)(n+1) f_{n,n+1}}{\epsilon_{n,n+1}} + (2\pi^2) \sum_{\lambda} V_{n\lambda} V_{\lambda,n+1} [f_{n\lambda}\delta(\epsilon_{n\lambda}) + f_{n+1,\lambda}\delta(\epsilon_{n+1,\lambda})] \times [|V_{n\lambda}|^2 \delta(\epsilon_{n\lambda}) + |V_{n+1,\lambda}|^2 \delta(\epsilon_{n+1,\lambda})] / \{\epsilon_{n,n+1}^2 + \pi^2 \textstyle\sum_{\lambda} [|V_{n\lambda}|^2 \delta(\epsilon_{n\lambda}) + |V_{n+1,\lambda}|^2 \delta(\epsilon_{n+1,\lambda})]^2\} \right] . \tag{4.6}$$

Let us look at the arguments of the energy δ functions in expressions (4.5) and (4.6) for the current

$$\epsilon_{n\lambda} = \epsilon_{n,k_y,k_z} - \epsilon_{n',k_y',k_z'} = \epsilon_{n\lambda}^0 - eE(x_0 - x_0') \quad . \tag{4.7}$$

In Eq. (4.7) we have made use of Eq. (3.6). We have also used the notation $\epsilon_{n\lambda}^0 = \epsilon_{n,k_z} - \epsilon_{n',k_z'}$. Upon substituting for x_0 and x_0' from Eq. (3.9), we find

$$\epsilon_{n\lambda} = \epsilon_{n\lambda}^0 - eE\lambda_m^2 Q_y \quad ,$$

where

$$Q_y = q_y + Dq_z \quad , \tag{4.8}$$

with

$$D = (\alpha_{11}\alpha_{23} - \alpha_{13}\alpha_{12})/(\alpha_{11}\alpha_{22} - \alpha_{12}^2) \quad .$$

The momentum transfer $k_y - k_y'$ in the y direction has been set equal to the phonon momentum q_y, because of the Kronecker δ's in Eq. (4.2). Similarly, $k_z - k_z' = q_z$. Using Eq. (4.8), we can interconnect $\delta(\epsilon_{n\lambda})$ and $\delta(\epsilon_{n\lambda}^0)$ by expanding with $eE\lambda_m^2 Q_y$ as the expansion parameter. The "smallness" of the parameter implies physically that the work done by the electric field over the magnetic length λ_m is small compared with the translational kinetic energy of the electron. By making the lowest-order expansion, our intent here is to reformulate the results for numerical application.

Upon using (4.8) in Eq. (4.5) together with the identities,[9]

$$\sum_{q_y} q_y V_{n\lambda} V_{\lambda,n+1} = (\sqrt{2}\,\beta\lambda_m^2)^{-1} (n+1)^{1/2} \sum_{\lambda} |V_{n\lambda}|^2 \quad , \tag{4.9}$$

$$\sum_{q_z} q_z V_{n\lambda} V_{\lambda,n+1} = (\sqrt{2}\,\beta\lambda_m^2)^{-1} (n+1)^{1/2} \sum_{\lambda} |V_{n\lambda}|^2 \quad ,$$

we find to first order in E

$$\langle j_x \rangle = \frac{e^2\hbar}{m} (1+D)\alpha_{11} E \sum_{n,k} \left[(n+1) \left(f'(\epsilon_n) \frac{\hbar}{\tau(n)} + \frac{f'(\epsilon_{n+1})\hbar}{\tau(n+1)} \right) \frac{\epsilon_{n,n+1}}{\epsilon_{n,n+1}^2 + \hbar^2/\tau_{n+1}^2} \right] , \tag{4.10}$$

where D is given by (4.8) and

$$\frac{1}{\tau_{n+1}} = \frac{1}{\tau(n)} + \frac{1}{\tau(n+1)} = \frac{\pi}{\hbar} \sum_{\lambda} [|V_{n\lambda}|^2 \delta(\epsilon_{n\lambda}^0) + |V_{n+1,\lambda}|^2 \delta(\epsilon_{n+1,\lambda}^0)] . \tag{4.11}$$

Here, the relaxation time $\tau(n)$ is defined by

$$1/\tau(n) = (\pi/\hbar)\sum_{\lambda} \left| V_{n\lambda} \right|^2 \delta(\epsilon^0_{n\lambda}) \ . \tag{4.12}$$

In like manner, we obtain

$$\langle j_y \rangle = \frac{e^2\hbar}{m} (\bar{\alpha}_{22}\alpha_{11})^{1/2} (1+D) E \sum_{n,k} (n+1) \times \left[\frac{f_{n,n+1}}{\epsilon_{n,n+1}} + \left(f'(\epsilon_n) \frac{\hbar}{\tau(n)} + f'(\epsilon_{n+1}) \frac{\hbar}{\tau(n+1)} \right) \times \left(\epsilon^2_{n,n+1} + \frac{\hbar^2}{\tau^2_{n+1}} \right)^{-1} \frac{\hbar}{\tau_{n+1}} \right] . \tag{4.13}$$

The results obtained here should be good for low magnetic fields ($\omega\tau \ll 1$) as well as high ($\omega\tau \gg 1$). This is made possible by the presence of the cutoff factor $1/(\epsilon^2_{n,n+1} + \hbar^2/\tau^2_{n+1})$. With $\epsilon_{n,n+1} = \hbar\omega^*$, the cutoff factor[16] is obtained in the form $1/(\omega^{*2} + 1/\tau^2_{n+1})$.

The relaxation time defined by Eq. (4.12) is obtained using Eqs. (4.2)–(4.4) as

$$\frac{1}{\tau(n)} = A \sum_{n'}{}' [\epsilon_n - (n' + \tfrac{1}{2}\hbar\omega^*]^{-1/2} \ . \tag{4.14}$$

Here,

$$A = \frac{2\pi E_1^2 kT (2\pi\lambda_m)^{-2} (2m^*/\hbar^2)^{1/2}}{\hbar\rho_d v_s^2}$$

characterizes the electron-phonon coupling in terms of the previously defined symbols. The prime on the summation is to remind us of the restriction $\epsilon_n \geq (n' + \frac{1}{2})\hbar\omega^*$ for values of n' included in the sum. For compactness, we define

$$\sum_1 = \sum_{n'}{}' [\epsilon_n - (n' + \tfrac{1}{2})\hbar\omega^*]^{-1/2} \ ,$$
$$\sum_2 = \sum_{n'}{}' [\epsilon_{n+1} - (n' + \tfrac{1}{2})\hbar\omega^*]^{-1/2} \ . \tag{4.15}$$

The electron distribution function $f(\epsilon_n)$ to be used in Eq. (4.10) will be taken to be the nondegenerate limit of the Fermi distribution,

$$f(\epsilon_n) = \exp[\mu - \epsilon_n)/kT] \ , \tag{4.16}$$

where μ is the Fermi energy in the presence of the magnetic field. The x component of the current then reads

$$\langle j_x \rangle = \frac{e^2\hbar\alpha_{11}E(1+D)}{m} \sum_{n,k} (n+1) \left(e^{(\mu-\epsilon_n)/kT} A \frac{\hbar\omega^*}{kT} \times [\sum_1 + e^{-\hbar\omega^*/kT} \sum_2] [(\hbar\omega^*)^2 + A^2(\sum_1 + \sum_2)^2]^{-1} \right) . \tag{4.17}$$

Equation (4.6) can be similarly rewritten in terms of $\sum_1$ and $\sum_2$. We omit most of the tedious but straightforward algebra required to reduce the sums defined above to a convenient form for computation. After this reduction, it is found that aside from some constant factor the expressions for current depend only on $\hbar\omega^{*3}/A^2 \propto B/T^2$ and $\hbar\omega^*/kT \propto B/T$.

In the case of acoustic-mode scattering, the zero magnetic field mobility is given by[14]

$$\mu_0 = \tfrac{2}{3}\sqrt{2}\,\pi^{1/2}\hbar^4\rho_d v_s^2 e/[E_1^2 m^{*5/2}(kT)^{3/2}] \ , \tag{4.18}$$

in terms of which $\hbar\omega^{*3}/A^2 = (9\pi m^2 k\omega^* T/4e^2\hbar)\mu_0^2$. For our numerical calculations on n-Ge, we used

$$\frac{(\hbar\omega^{*3}/A^2)}{(\hbar\omega^*/kT)} = \frac{(266)^2}{T(^\circ\mathrm{K})}$$

to agree with zero magnetic field experimental results.[1,17] The α-tensor components of Sec. III were found using[14]

$$\alpha_1 = m/m_t = 1/0.082 \quad \text{and} \quad \alpha_3 = m/m_l = 1/1.58 .$$

The expression (4.17) for the current involves the Fermi energy μ. In finding μ in high magnetic fields, the interaction energy between the electron's magnetic moment and the magnetic field may be important.[18] This involves the effective g factor of electrons in the conduction band which is anisotropic in germanium. The spin-magnetic field interaction where the g factor is anisotropic and is therefore a tensor is given by[19,20] $V_s = \frac{1}{2}\mu_B \vec{\sigma}^P \cdot \overleftrightarrow{g} \cdot \vec{B}$ where $\vec{\sigma}^P$ stands for the Pauli-spin matrices. The g-tensor components are calculated along the same lines as the α-tensor components using[20] $g_1 = 1.92$ and $g_{33} = g_3 = 0.87$. The total number of electrons $N(B)$ in the conduction band is then found to be

$$N(B) = \sum_{\sigma=1} N_\sigma(B) = \sum_{\sigma=1} \left[2(2\pi\lambda_m)^{-2} \exp\left(\frac{\mu}{kT}\right) \times \cosh \frac{\mu_B B}{kT} \left(g_{13}^{(\sigma)2} + g_{23}^{(\sigma)2} + g_{33}^{(\sigma)2} \right)^{1/2} \times \left(\frac{2\pi m_\sigma^* kT}{h^2} \right)^{1/2} \mathrm{cosech}\left(\frac{\hbar\omega_\sigma^*}{kT} \right) \right] . \tag{4.19}$$

The ellipsoid index σ has been restored here for clarity. In this expression the hyperbolic cosine term arises from the Boltzmann factor for the two spin orientations. The remaining factors in Eq. (4.19) are obtained from the rest of the Boltzmann factor by summing over the energy eigenstates. The current components were then calculated for each ellipsoid and summed over the four ellipsoids. The conductivity components σ_{ij} were then obtained using $j_i = \sigma_{ij}E_j$.

In the presence of a magnetic field in the z direction and a current in the x direction with the electric field in the xy plane, what is frequently

measured experimentally is the magnetoresistance ratio $\rho_{xx}(B)/\rho(0)$ and the Hall voltage (ρ_{xy}). The ρ_{ij}'s stand for the resistivity-tensor components in the laboratory frame and $\rho(0)$ is the resistivity in zero magnetic field. The resistivity-tensor components are found by inverting the conductivity tensor. This yields

$$\rho_{xx} = \sigma_{xx}/(\sigma_{xx}^2 + \sigma_{xy}^2)$$

if the current and the magnetic field are in symmetry directions. In our calculations we used the $T^{3/2}$ law for acoustic scattering to calculate $\rho(0)$ at various temperatures, starting with the experimentally measured value[1] of $\rho(0)$ at $T = 77\,^{\circ}\mathrm{K}$,

$$\rho^T(0) = (4\Omega - \mathrm{cm})\,(T/77)^{3/2}\,.$$

The following geometries were investigated: $\vec{B}$ in the (1, 0, 0) direction with J in the (0, 0, 1) direction; B in the (1, 1, 0) direction with J in the (1, −1, 0) direction; and B in the (1, 1, 1) direction with J in the (1, −1, 0) direction. The calculations were made for an electron concentration of $10^{14}\,\mathrm{cm}^{-3}$. All data were processed using the University of Colorado CDC 6400 computer.

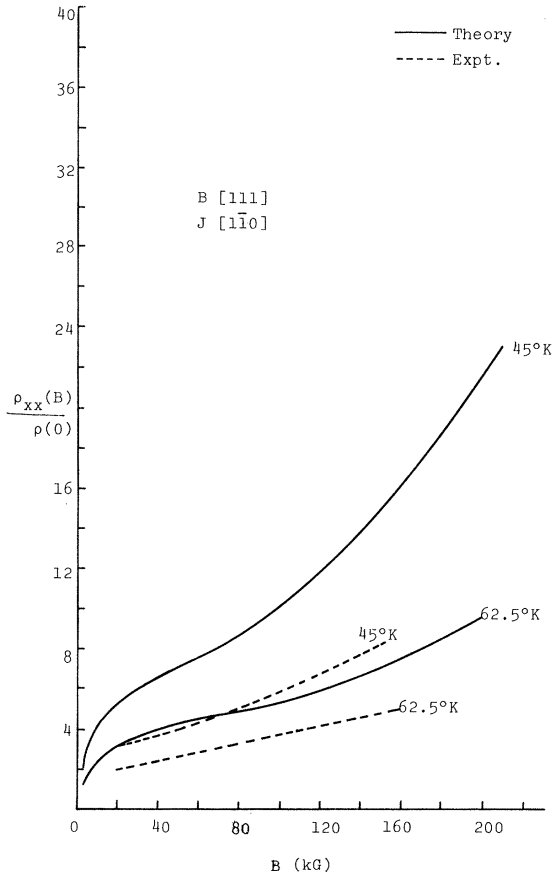

FIG. 1. Transverse magnetoresistance of n-Ge for various temperatures and symmetry directions. The solid curves are the theoretical ones and the dashed curves are from the experiments of Gallagher and Love, Ref. 1.

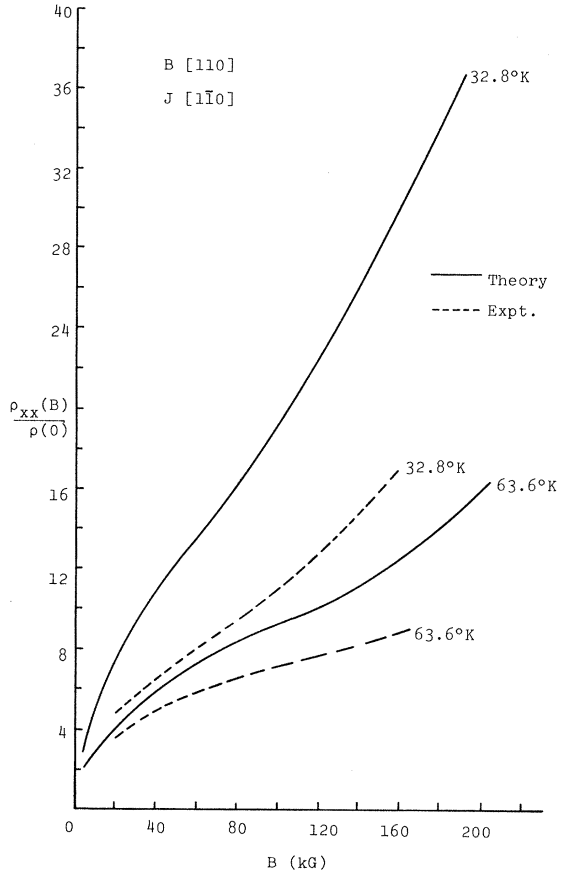

FIG. 2. Transverse magnetoresistance of n-Ge for various temperatures and symmetry directions. The solid curves are the theoretical ones and the dashed curves are from the experiments of Gallagher and Love, Ref. 1.

V. RESULTS AND DISCUSSION

Numerical results for several temperatures in the range $T = 30$–$77\,^{\circ}\mathrm{K}$ are depicted graphically (Figs. 1–3) in the plots of $\rho_{xx}(B)/\rho(0)$ versus B for magnetic fields up to 200 kG. In all these figures the solid lines are the theoretical curves, while the dashed lines refer to the experimental data of Gallagher and Love.[1] The theoretical curves for higher T continue to rise in the 20–100-kG region and do not exhibit a true saturation region as predicted by theories based on the concept of a fixed relaxation time. Thus the variation of relaxation time with magnetic field tends to wipe out the saturation region. The curves have steeper slopes at higher fields and lower

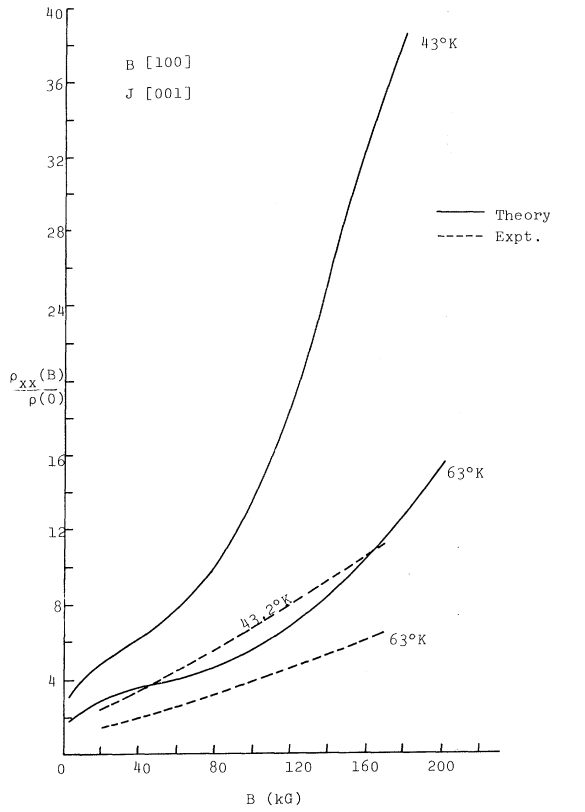

FIG. 3. Transverse magnetoresistance of n-Ge for various temperatures and symmetry directions. The solid curves are the theoretical ones and the dashed curves are from the experiments of Gallagher and Love, Ref. 1.

temperatures. The inflection is pronounced at the lower temperatures. It is clear from the figures that there is not quantitative agreement with experiment at higher magnetic fields. This is surprising in view of the Miller and Omar[13] calculations on longitudinal magnetoresistance using acoustic-phonon scattering. Their results indicate agreement with experiment[21] to better than 10%, showing that for $\vec{J}$ parallel to $\vec{B}$ this scattering mechanism is dominant.

The experimental data show a near linear variation with magnetic field at low temperatures. Many investigators have attributed this lack of saturation of magnetoresistance to inhomogeneities or surface effects. One is also tempted to blame such effects for the lack of quantitative agreement between theory and experiment. However, Puri[22] points out that while surface effects change the magnitude of $\rho_{xx}(B)$ a little, the field dependence is nearly the same for a sand blasted or etched sample. Gallagher and Love[1] questioned the possibility of detecting randomly distributed inhomogeneities by measuring $\rho_{xx}(B)/\rho(0)$ as a function of B. Also, as pointed out previously, the extensive investigations of Baranskii and Babich[2] showed very little correlation between inhomogeneities and the magnitude of the near linear rise of magnetoresistance with B. They conclude very firmly that the linear behavior is entirely due to quantization effects. In addition, the most recent results of Orazgulyev[23] on the transverse magnetoresistance in n-Si show that approach to saturation is not observed for $T < 150\,^{\circ}$K. He remarks that quantum effects mask the magnetoresistance saturation. The disagreement between theory and experiment in the transverse magnetoresistance suggests that the crossed $\vec{E}$ and $\vec{B}$ fields introduce a new relaxation process in addition to the magnetic-field-dependent acoustic phonon τ we have considered here. It is planned to investigate this possibility in future studies.

---

†Work supported in part under Grant No. NONR 1147 12 of the U. S. Navy.

*This paper is based in part on a Ph. D. dissertation submitted by one of us (P. K. G.) to the University of Colorado, Boulder, Colo., 1970.

‡Present address: Department of Electrical Engineering, University of Colorado, Boulder, Colo. 80302.

[1]J. W. Gallagher and W. F. Love, Phys. Rev. 161, 793 (1967).

[2]P. I. Baranskii and V. M. Babich, Fiz. Tekh. Poluprov. 3, 689 (1969) [Soviet Phys. Semicond. 3, 586 (1969)].

[3]E. N. Adams and T. D. Holstein, J. Phys. Chem. Solids 10, 254 (1959).

[4]P. N. Argyres and L. M. Roth, J. Phys. Chem. Solids 12, 89 (1959).

[5]R. Kubo, H. Hasegawa, and N. Hashitsume, J. Phys. Soc. Japan 14, 56 (1959).

[6]R. Kubo, N. Hashitsume, and S. J. Miyake, Solid State Phys. 17, 269 (1966).

[7]A. M. Kosevich and V. V. Andreev, Zh. Eksperim. i Teor. Fiz. 38, 882 (1960) [Soviet Phys. JETP 11, 637 (1960)].

[8]M. I. Klinger, Fiz. Tverd. Tela 3, 1342 (1961) [Soviet Phys. Solid State 3, 974 (1961)]; *ibid.* 3, 2507 (1961) [*ibid.* 3, 1824 (1962)].

[9]P. N. Argyres, Phys. Rev. 117, 315 (1960).

[10]H. Brooks, Advan. Electron. Electron Phys. 7, 85 (1955).

[11]H. Goldstein, *Classical Mechanics* (Addison-Wesley, Reading, Mass., 1956).

[12]P. P. Debye and E. M. Conwell, Phys. Rev. 93, 693 (1954).

[13]S. C. Miller and M. A. Omar, Phys. Rev. 123, 74 (1961).

[14]E. M. Conwell, *Solid State Physics*, edited by F. Seitz and D. Turnball (Academic, New York, 1967), Suppl. 9.

[15]W. Shockley and J. Bardeen, Phys. Rev. 80, 72

(1950). Apparently, it is not obvious that the simple scalar deformation potential model of Shockley and Bardeen is adequate. One should, in principle, formulate V in terms of a deformation-potential tensor. However, the effect of anisotropy is not large: $\sim 1.5\%$ (see e.g., Ref. 14, p. 115). In any case, the value of E_1 in our case is determined by the zero magnetic field experimental results. [See text following Eq. (4.18)].

[16]R. Kubo *et al.* (Ref. 6) have given a treatment of collision broadening and have compared this with the cutoff due to inelasticity. From these calculations, it may be verified that inelasticity of acoustic-phonon scattering would be present at sufficiently low temperatures (~ 15 °K) while collision broadening is ineffective, except at very high temperatures (>100 °K) and very high magnetic fields (>300 kG). In the 30-77 °K, 0-200-kG region of interest to us, the cutoff factor found naturally in the theory should be adequate for strong as well as weak magnetic fields. The present theory can be extended to inelastic phonon scattering as well.

[17]C. Herring *et al.*, J. Phys. Chem. Solids 18, 139 (1961).

[18]D. F. Minner, Ph. D. thesis, University of Colorado, 1963 (unpublished).

[19]L. M. Roth, Phys. Rev. 118, 1554 (1960).

[20]D. K. Wilson and G. Feher, Bull. Am. Phys. Soc. 5, 60 (1960).

[21]W. F. Love and W. F. Wei, Phys. Rev. 123, 67 (1961).

[22]S. M. Puri, Ph. D. thesis, Columbia University 1964 (unpublished).

[23]B. Orazgulyev, Fiz. Tekh. Poluprov. 3, 1425 (1969) [Soviet Phys. Semicond. 3, 1196 (1970)].

PHYSICAL REVIEW B VOLUME 2, NUMBER 8 15 OCTOBER 1970

Quantum Oscillations of Microwave Helicon Dispersion in n-Type InSb and InAs†

J. K. Furdyna and A. R. Krauss
Department of Physics, Purdue University, Lafayette, Indiana 47907

(Received 20 February 1970)

The effect of orbital quantization on microwave helicon dispersion in n-type InSb and InAs is investigated theoretically and experimentally. In the local limit, the leading term describing helicon dispersion is, unlike helicon damping, unaffected by orbital quantization. Quantum effects enter through the *scattering-dependent* terms involved in the dispersive part of the helicon propagation constant. The main contribution is shown to be associated with the Shubnikov–de Haas-like oscillations of the scattering correction to the dissipationless Hall conductivity. Experimental measurements of the transmitted helicon phase observed at quantizing magnetic fields in highly doped n-type InSb and InAs at 35 GHz and liquid-helium temperature are compared with the theory. The magnetic field dependence of the observed oscillations in helicon phase agrees reasonably well with the theoretical analysis. While little can be said analytically about the amplitude of these oscillations (of the order of a few percent), our data does provide an empirical measure of the limits within which the usual classical analysis of helicon dispersion is valid. Finally, the effect of quantum oscillations appears to be considerably stronger in the helicon dispersion than in the related dc problem of the Hall coefficient.

INTRODUCTION

It is well known that in the quantum limit helicon-wave damping in semiconductors and semimetals displays strong Shubnikov–de Haas-like oscillations. [1,2] At the same time it is usually assumed that helicon *dispersion* is free of the effects of orbital quantization. Of course, this is an approximation, since both damping and dispersion originate in the same conductivity tensor. The behavior of helicon damping and dispersion is similar, respectively, to the behavior of transverse dc magnetoresistance and Hall effect. While in magnetoresistance the Shubnikov–de Haas oscillations are overwhelming, the Hall coefficient is relatively independent of these contributions. Nevertheless, weak quantum oscillations in the Hall effect in semiconductors have been known qualitatively for some 15 years [3] and have more recently been a subject of quantitative experimental as well as theoretical study. [4,5]

In this paper we investigate the oscillatory magnetic field dependence of the local helicon-wave dispersion in small-gap semiconductors in the quantum limit. In order to determine the dominant oscillatory contributions to the helicon dispersion, we analyze the general expression for transmitted helicon phase in the light of existing theoretical formulations of the appropriate quantum conductivity tensor. Specifically, it is shown that, in the parameter range of interest, oscillatory contributions to the helicon dispersion originate primarily in the *frequency-independent* elements of the local conductivity tensor and are dominated by the small